钛合金表面反应电火花沉积 TiN/Ti 复合涂层

郝建军[1,2]，　彭海滨[1]，　黄继华[3]，　马跃进[1]，　李建昌[1]

（1. 河北农业大学 机电工程学院，河北 保定　071001；
2. 河北省轻金属材料工程技术研究中心，河北 保定　071000；
3. 北京科技大学 材料科学与工程学院，北京　100083）

摘　要：利用自制的电火花沉积充气密闭式保护装置和 DZ — 1400 型电火花沉积/堆焊机，以工业纯钛 TA2 为电极，以工业纯氮为保护气和反应气，在 TC4 钛合金表面上反应电火花沉积制备了 TiN/Ti 复合涂层. 利用扫描电子显微镜（SEM）、X 射线衍射仪（XRD）、X 射线光电子仪（XPS）分析了涂层的组织、物相和元素组成，利用显微硬度计测定了涂层的显微硬度，利用自制磨损试验装置对比涂层与淬火 W18Cr4V 高速钢的磨损性能. 结果表明，涂层与基体形成良好的冶金结合，涂层主要由钛和反应合成的 TiN 组成，涂层的平均显微硬度可达 1 388 HV0.1，是基体硬度的 6 倍以上，涂层具有较好的耐磨性.

关键词：反应电火花沉积；氮化钛；复合涂层；钛合金
中图分类号：TG174.453　　文献标识码：A　　文章编号：0253－360X(2009)11－0069－04

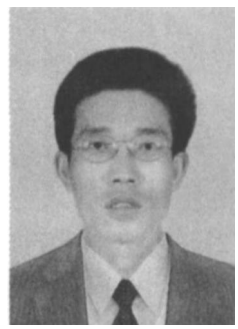

郝建军

0　序　　言

TiN 金属陶瓷材料因其高强度、高硬度、耐高温、耐酸碱侵蚀、耐磨损以及良好的导电性、导热性等一系列优点而广泛用于切削刀具、抗磨粒磨损和磨蚀磨损零部件的表面强化. 目前，研究人员对 TiN 涂层制备方法、工艺、设备及机理的研究多集中在物理气相沉积（PVD）法、化学气相沉积（CVD）法、激光表面气体合金化法、等离子喷涂等技术上[1－3]. 上述技术需要昂贵的设备、特定的场所、专业的技术人员，从而使 TiN 涂层制备成本大大增加，限制了其在工业上的广泛应用.

反应电火花沉积工艺是一种脉冲微弧焊接过程，它将电源存储的高能量电能在电极与基体间瞬间高频释放，使电极与基体之间产生高温、高压微区的同时将作为反应组元的保护气体击穿电离，同时离子态的电极材料、基体材料与反应组元保护气体发生化合反应，电极材料和生成的新相在微电场的作用下熔渗到基体表面，形成合金化的表面沉积层，从而使工件的物理性能、化学性能和力学性能得到显著改善.

文中针对常规 TiN 制备中存在工艺复杂、成本高、厚度小等问题，采用反应电火花沉积合成技术[4]，采用自制的电火花沉积充气密闭式保护装置，以工业纯钛 TA2 为电极材料，以工业纯氮为保护气体和反应气体，在 TC4 钛合金基体表面上制备了 TiN 增强金属基复合涂层，并对涂层物相、显微组织、化学组成、硬度和耐磨性能进行了初步分析.

收稿日期：2008－09－08
基金项目：河北省自然科学基金资助项目（E2007000566）

1　试验方法

电极材料为 φ3 mm 的工业纯钛 TA2. 试验试件材料为 TC4 钛合金，试件尺寸为 φ3 mm×1 mm 的圆形试样. 采用纯度大于 99.5% 的工业氮气作为保护气体和反应组元气体.

试验设备采用自制的电火花沉积充气密闭式保护装置[5]和中国农机院表面工程技术研究所研制生产的 DZ — 1400 型电火花沉积/堆焊机. 用 200 目砂纸打磨试件和电极表面以去除氧化皮，用浓度为 99.5% 的丙酮溶液清洗上述两表面以去除油污，自然干燥 5 min 后进行沉积试验. 沉积工艺参数为输出电压 90 V，电容量 80 μF，放电频率 700 Hz，电极转速 4 800 r/min，氮气流量 10 L/min，比沉积时间 3 min/cm^2.

沉积结束后，试件金相制样后采用 KyKy — 2800 型扫描电镜（SEM）观察涂层表面形貌和截面显微组织，采用 D/max — RA 型 X 射线衍射仪（XRD）

对涂层物相进行分析，采用 PHI Quantera SXM 型 X 射线光电子仪（XPS）对涂层表面元素进行分析，采用 MH －6 型显微硬度计测定沉积层的显微硬度，用自制磨损试验装置对比涂层与淬火 W18Cr4V 高速钢的磨损性能[6]．

2 试验结果与分析

2.1 涂层物相

试样经电火花沉积后，先对试样进行清洗，然后对试样作 X 射线衍射分析，图 1 为涂层的 XRD 分析结果．从图 1 可知，沉积层主要由 TiN 相、Ti_2N 相和 Ti 相组成．分析认为，涂层中 TiN 和 Ti_2N 相的形成是由于在电火花沉积过程中，旋转电极和基体之间产生脉冲微弧放电瞬时释放的能量将电极和基体材料熔化（甚至气化）的同时将部分氮气离子化为原子和离子状态．熔化的电极和基体形成熔池，具有高活性的氮（包括 N 离子、N 原子及未被电离的 N 分子）吸附在熔池表面，并通过扩散作用克服固液界面表面能进入熔池与部分熔融状态的钛反应形成 TiN 和 Ti_2N．涂层中钛相一部分来自熔池中与氮反应后的剩余钛，另一部分来自于因电极粘连[7] 和基体材料向涂层扩散所致．

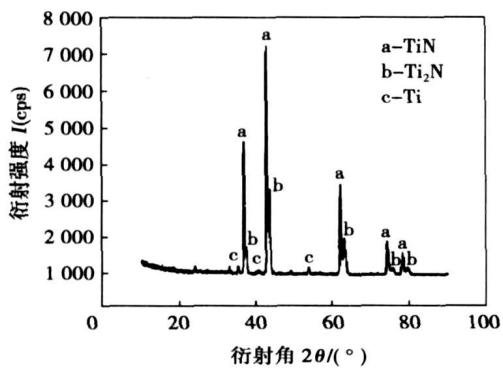

图 1 涂层 X 射线衍射图谱

Fig 1 XRD spectrum of coatings

2.2 涂层表面及截面形貌

图 2a 是试样涂层外观形貌．由图可以清晰地看到涂层呈桔皮状，宏观呈现为 TiN 特有的金黄色．该表面的形成是多次放电所形成的强化点的熔合和重叠的结果，这种表面形貌有利于储存润滑油并减少摩擦．

图 2b 是单脉冲强化点形貌．由图可以清晰地看到单脉冲强化点的直径约为 1.5 mm，强化点呈不规则的溅射状，并且存在较多呈颗粒状（A）、不规则的块状（B）和针状（C）的飞溅物，强化点中间凹陷成微坑且在坑底呈撕裂特征．分析认为，溅射状的形成是由于在脉冲放电过程中熔化的电极端部在高温高压条件下被高活性的氮（包括 N 离子、N 原子及未被电离的 N 分子）加速，撞击在基体表面形成；裂纹为沉积过程中电极粘连和内应力释放所致．

图 2c 是多脉冲强化点形貌．由图可以清晰地看到它保留了单脉冲强化点的部分特征，但与单脉冲相比较，多脉冲强化点坑底部较平坦，这是由于随着脉冲放电次数的增加，电极材料和反应生成物不断填入熔坑覆盖基体材料，致使电极与基体间的粘连作用减弱．另外，随着强化点面积的不断扩大，电极材料在熔坑边缘的飞溅物相互重叠，富积程度明显增加．

图 2d 为涂层表面形貌．由图可以看出，涂层表面比较平坦，但其上存少量气孔（A）和微裂纹（B），气孔是由强化点不连续形成的，微裂纹是由于循环热应力形成的．沉积层表面形貌仍能清晰地观察到单脉冲强化点的形貌．

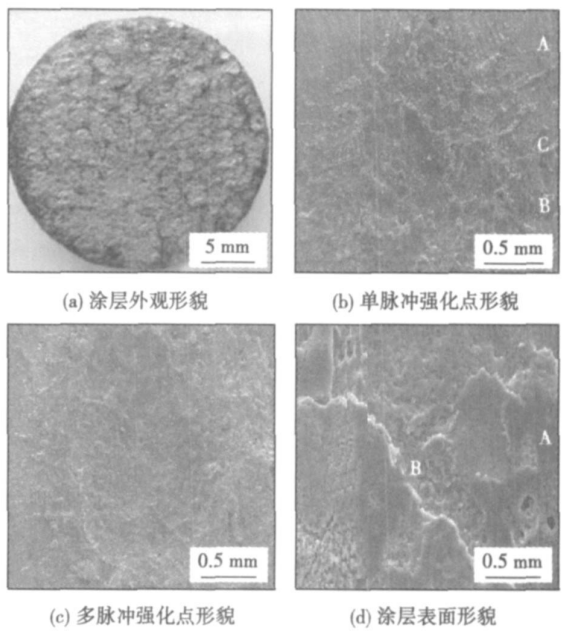

图 2 涂层表面特征

Fig 2 Characteristics of coatings surface

图 3 为试件横截面微观组织形貌．由图 3a 可以看出，试件断面可明显分成涂层区、过渡区、基体区 3 个区域，3 个区之间没有明显界限，结合致密．

图 3b 为图 3a 中涂层过渡区局部高倍微观组织形貌．由图可看出电极材料和反应生成物与基体材料间相互熔渗扩散，沉积层与基体之间形成冶金结合．

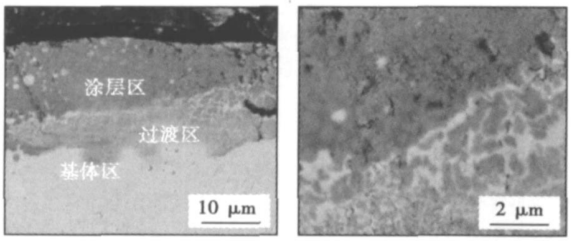

(a) 涂层截面微观组织形貌　　(b) 过渡区微观组织形貌

图 3　试件截面微观组织形貌

Fig. 3　Microstructure of cross section of specimen

2.3　涂层表面元素分析

涂层表面 XPS 全谱分析如图 4 所示. 由图可知，涂层中含有 O, C, Ti, N, Al 元素. 分析认为 Al 元素是因电极粘连作用由基体过渡到沉积层所致，C, O 元素来自沉积层表面吸附的 O_2, CO_2, 水分或尘埃（由于试验中未进行 Ar^+ 枪刻蚀）. 另外，由图 4 可知处于 396.68 eV 的峰（Ti-N 键的 N 1s）与文献[8] 的研究结果一致（文献[8] 的研究证实了结合能处于 396.7 eV ±0.1 eV 的 Ns1 峰表示理想配比的 TiN），这充分说明涂层中 N 元素与 Ti 元素化合，主要以氮化物（TiN）的形式存在，而不是以间隙原子的形式与钛形成固溶体.

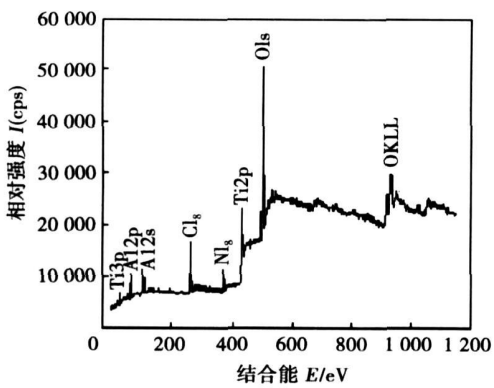

图 4　涂层表面 XPS 全谱图

Fig. 4　XPS complete spectrum of coatings surface

2.4　涂层显微硬度

图 5 为涂层截面显微硬度分布曲线. 由图可知，涂层表层的显微硬度最高达 1 388 HV0.1，是基体硬度（220 HV0.1）的 6 倍以上，这主要是由于涂层中有较多的 TiN 硬质相；而过渡区硬度已下降至 500 HV0.1 以下，这主要是由于过渡区中 Ti 元素含量增多、存在微裂纹和重复涂敷的回火作用等原因所致.

图 6 为涂层与对比试样（淬火 W18Cr4V 高速钢）在相同条件下磨损体积随载荷变化的关系曲线. 由图可以看出，在低载荷下涂层与对比试样的磨损量比较接近；随着载荷的增加，对比试样的磨损量远比涂层的高，当载荷达到 1 600 N 时，对比试样的磨损量达到了涂层的 2 倍. 分析认为，反应生成的 TiN 相中存在 N 元素的缺位，使 TiN 的金属性增强，涂层韧性增强，从而提高了涂层的使用寿命.

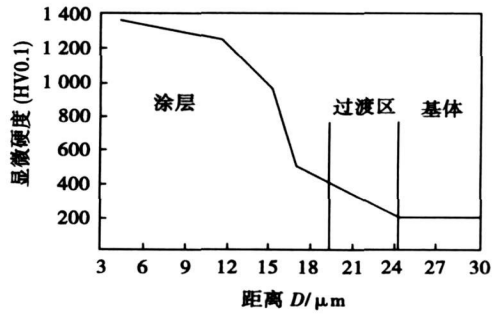

图 5　涂层显微硬度分布曲线

Fig. 5　Microhardness profile of coatings

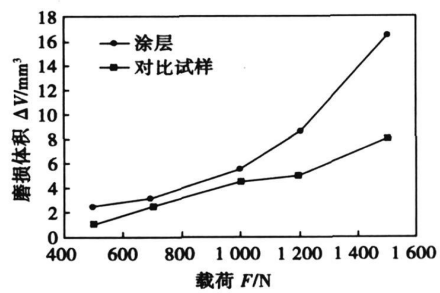

图 6　涂层与淬火 W18Cr4V 高速钢磨损体积对比

Fig. 6　Contrast of lost volume for coatings and W18Cr4V

3　结　　论

（1）利用电火花沉积技术，以工业纯钛 TA2 为电极，氮气为反应及保护气体，在 TC4 钛合金表面制备出了含 TiN 硬质相的致密、均匀、连续的反应涂层.

（2）涂层主要由 TiN 相、Ti_2N 相和钛相组成，TiN 和 Ti_2N 相是在高温条件下，熔融的金属钛与 N 离子、N 原子及 N 分子发生反应生成.

（3）涂层硬度随着到表面距离的增大而减小，显微硬度最高达 1 388 HV0.1，是基体硬度的 6 倍多.

（4）涂层与基体形成冶金结合，涂层中 TiN 相

中存在N元素的缺位,使TiN的金属性增强,涂层韧性增强,涂层耐磨性良好.

(5)文中涉及的反应电火花沉积TiN/Ti复合涂层,方法简单、制备效率高、涂层硬度高、韧性好,从根本上解决了常规制备TiN涂层工艺复杂、成本高、厚度小等问题,降低了TiN的制备成本,拓展了TiN涂层的工业制备途径.

参考文献:

[1] 于 翔, 王成彪, 刘 阳, 等. 中频对靶磁控溅射合成TiN/Ti多层膜[J]. 金属学报, 2006, 42(6): 662—666.
Yu Xiang, Wang Chengbiao, Liu Yang, *et al*. TiN/Ti multilayer films synthesized by mid-frequency dual-magnetron sputtering [J]. Acta Metallurgica Sinica, 2006, 42(6): 662—666.

[2] 马大衍, 马胜利, 徐可为, 等. 残余氧对TiN+Si_3N_4纳米复合薄膜硬度的影响[J]. 金属学报, 2004, 40(10): 1037—1040.
Ma Dayan, Ma Shengli, Xu Kewei, *et al*. Impact of residual oxygen on hardness of nano structured TiN+Si_3N_4 film [J]. Acta Metallurgica Sinica, 2004, 40(10): 1037—1040.

[3] 于永泗, 赵 群, 张立文, 等. 钛合金激光渗氮层的组织与性能研究[J]. 金属热处理, 2003, 28(12): 21—24.
Yu Yongsi, Zhao Qun, Zhang Liwen, *et al*. Structure and property of nitriding layer on titanium alloy by laser[J]. Heat Treatment of Metals, 2003, 28(12): 21—24.

[4] 郝建军, 马跃进, 陈志强, 等. 一种氮化钛金属基陶瓷涂层的反应电火花沉积制备方法: 中国, CN200610012842.4[P]. 2006—11—22.

[5] 郝建军, 马跃进, 陈志强, 等. 电火花沉积充气密闭式气体保护及供给装置: 中国, CN200620024726.X[P]. 2007—09—05.

[6] 郝建军, 马跃进, 杨 欣, 等. 火焰熔覆镍基/铸造碳化钨熔覆层在犁铧上的应用[J]. 农业机械学报, 2005, 36(11): 145—148.
Hao Jianjun, Ma Yuejin, Yang Xin, *et al*. Experimental investigation on plowshare coated by flame cladding Ni-base cast WC[J]. Transactions of the Chinese Society of Agricultural Machinery, 2005, 36(11): 145—148.

[7] 何 鹏, 吴承东, 钱乙余, 等. 钛合金表面电火花沉积WC电极的粘连行为分析[J]. 焊接学报, 2006, 26(4): 28—31.
He Peng, Wu Chengdong, Qian Yiyu, *et al*. Adhesion behavior of WC coating deposited on titanium alloy by electrospark deposition[J]. Transactions of the China Welding Institution, 2006, 26(4): 28—31.

[8] Bertoti I, Mohai M, Sullivan J L, *et al*. Surface characterisation of plasma-nitrided titanium: an XPS study[J]. Applied Surface Science, 1995, 84(4): 357—371.

作者简介: 郝建军, 男, 1972年出生, 博士, 副教授. 主要从事材料表面改性及表面涂层制备方面的研究与教学工作. 发表论文40余篇.

Email: hjjpaper@163.com

[上接第68页]

结构发生热疲劳失效的电阻值经验判据,锡铅钎料焊点发生热疲劳失效的电阻值为1.068(归一化结果);无铅钎料SAC305焊点的电阻值为1.090(归一化结果).

参考文献:

[1] 李恒德, 马春来. 材料科学与工程国际前沿[M]. 济南: 山东科学技术出版社, 2002.

[2] 黄 萍. 焊点的失效模式与分析[J]. 电子工艺技术, 2006, 27(4): 205—208.
Huang Ping. Analysis of the failure mode of solder joint[J]. Electronics Process Technology, 2006, 27(4): 205—208.

[3] Mutoh Y, Zhao J, Miyashita Y, *et al*. Fatigue crack growth behavior of lead-containing and lead-free solders [J]. Soldering and Surface Mount Technology, 2002, 14(3): 37—45.

[4] 颜秀文, 丘 泰, 张振忠. 无铅电子封装材料及其焊点可靠性研究进展[J]. 电子元件与材料, 2006, 25(3): 5—8.
Yan Xiuwen, Qiu Tai, Zhang Zhenzhong. Research progress of lead-free solders and solder joint reliability in electronic packaging[J]. Electronic Components and Materials, 2006, 25(3): 5—8.

[5] Wang G Z, Zhu Q N, Cheng Z N, *et al*. Solder joint geometry of tin-lead alloy and its application in electronic packaging[J]. Transactions of Nonferrous Metals Society of China, 1999, 9(4): 733—740.

[6] Wang G Z, Fang H Y, Wang C Q, *et al*. An experimental study of effect of solder joint geometry on thermal cycle life in SMT[J]. China Welding, 1997, 6(1): 67—73.

[7] Shangguan D K. Analysis of crack growth in solder joints[J]. Soldering &Surface Mount Technology, 1999, 11(3): 27—32.

[8] Tu P L, Chan Y C, Lai J K L. Effect of intermetallic compounds on the thermal fatigue of surface mount solder joints[J]. IEEE Transactions on Components, Packaging and Manufacturing Technology, Part B: Advanced Packaging, 1997, 20(1): 87—93.

[9] Liu X S, Lu G Q. Effects of solder joint shape and height on thermal fatigue lifetime[J]. IEEE Transactions on Components and Packaging Technologies, 2003, 26(2): 455—465.

作者简介: 林 健, 男, 1979年出生, 博士, 助理研究员. 主要从事电子电路中焊点可靠性方面的科研与教学工作. 发表论文20余篇.

Email: linjian@bjut.edu.cn

shaped and the thickness of IMC is much thinner when SAC0307 solder added 0.05% Ni is used. The consumption of Ni layer is nearly the same using both solders after the first time reflow soldering, but the residual thickness of the Ni layer in SAC0307/Ni solder is thinner than that in SAC0307-0.05Ni/Ni after aging for 384 h. So solders with a little Ni element can decrease the consumption rate of Ni layer effectively during aging, that is, the aging-resistant ability of Ni pad is improved obviously.

Key words: SAC0307-*x*Ni; solder; Ni substrate; IMC; aging

Wettability of molten $Zr_{55}Al_{10}Ni_5Cu_{30}$ metallic glass brazing alloy on α-Al_2O_3 and ZrO_2 ZHENG Xiaohong, SHEN Ping (Key Laboratory of Automobile Materials Ministry of Education, Jilin University, Changchun 130025, China). p 57—60, 64

Abstract: The wettability and interfacial characteristics of molten $Zr_{55}Al_{10}Ni_5Cu_{30}$ metallic glass brazing alloy on polycrystalline α-Al_2O_3 and ZrO_2 substrates were studied using a modified sessile drop method. The results show that the wettability of the $Zr_{55}Al_{10}Ni_5Cu_{30}$/$\alpha$-$Al_2O_3$ system is excellent with the final contact angles approaching zero degree at 1 133-1 193 K. However, the wettability of the $Zr_{55}Al_{10}Ni_5Cu_{30}$/$ZrO_2$ system is poor, but it can be progressively improved with the elapse of time during the isothermal dwelling in the temperature range of 1 133-1 253 K. A certain extent of interfacial reaction happens in both systems. The investigation on the spreading kinetics and interfacial microstructure indicates that the adsorption of the active atoms such as Zr at the interface, particularly at the triple junctions, plays a key role in determining the wettability, whereas the contribution of the interfacial reaction is relatively minor.

Key words: Metallic glass brazing alloy; wettability; interfacial reaction; adsorption

Microstructure and mechanical properties of magnesium alloy AZ31B joint brazed with Al-Mg-Zn filler metal MA Li[1], HE Dingyong[1], LI Xiaoyan[1], JIANG Jianmin[1], WANG Lizhi[2] (1. College of Materials Science and Engineering, Beijing University of Technology, Beijing 100124, China; 2. Welding Research Institute of Central Research Institute of Building & Construction, China Metallurgical Group Corporation, Beijing 100088, China). p 61—64

Abstract: High-frequency induction brazing of wrought magnesium alloy AZ31B with Al-Mg-Zn filler metal was investigated. Microscopic structure, the phases and the mechanical properties of brazed joint were studied. The microstructure and formation phases at the interface in the brazed joint were investigated by scanning electron microscopy (SEM), X-ray diffraction instrument (XRD) and energy dispersive spectrometer (EDS). The strength of the brazed joint and the microhardness of the formation phases were also tested. The results show that, Al-Mg-Zn filler metal reacting with the base metal AZ31B, and α-Mg+β-$Mg_{17}(Al, Zn)_{12}$ divorced eutectic structure is formed in the brazed joint. Microhardness of the base metal AZ31B is the smallest and β-$Mg_{17}(Al, Zn)_{12}$ phase of the brazed joint is the hardest. Both the butt joint and the overlap joint exhibit intergranular fracture mode, the fracture comes from hard brittle phase β-$Mg_{17}(Al, Zn)_{12}$ of α-Mg+β-Mg17$(Al, Zn)_{12}$ divorced eutectic structure.

Key words: AZ31B magnesium alloy; Al-Mg-Zn filler metal; brazing; divorced eutectic; joint strength

Failure of soldered joint during thermal fatigue test LIN Jian[1], LEI Yongping[1], ZHAO Haiyan[2], WU Zhongwei[1] (1. College of Materials Science and Engineering, Beijing University of Technology, Beijing 100124, China; 2. Department of Mechanical Engineering, Tsinghua University, Beijing 100084, China). p 65—68, 72

Abstract: The failure process of soldered joint in SMT was investigated by electrical resistance measurement method and crack observation method. The characteristics of electrical resistance value variation of lead-tin and lead-free soldered (SAC305) joints during the thermal fatigue test were obtained. And at the same time the crack propagation in soldered joint was observed. According to these measurements, the failure rules of lead-tin and lead-free soldered joint were compared. The relationship between electrical resistance value variation and crack propagation of soldered joint during thermal fatigue test was studied by FEM, and an empirical criterion to estimate the failure of the soldered joint in the thermal fatigue test was obtained based on electrical resistance value variation. The experimental results show that the lead-free soldered joint has a higher resistibility in thermal fatigue than the traditional lead-tin soldered joint. The criterion based on electrical resistance value variation was founded from the experimental and simulation results.

Key words: SMT; soldered joint; thermal fatigue; electrical resistance; crack

TiN/Ti composite coating deposited on titanium alloy substrate by reactive electric-spark HAO Jianjun[1,2], PENG Haibin[1], HUANG Jihua[3], MA Yuejin[1], LI Jianchang[1] (1. College of Electromechanical Engineering, Agriculture University of Hebei, Baoding 071001, Hebei, China; 2. Light Metal Materials Engineering Research Center of Hebei, Baoding 071000, Hebei, China; 3. School of Materials Science and Engineering, University of Science and Technology of Beijing, Beijing 100083, China). p 69—72

Abstract: TiN/Ti composite coating was deposited on TC4 titanium alloy substrate with the self-made special gas-filled-closed electric-spark deposition device and electric-spark deposition machine modeled DZ-1400, the industry pure titanium (TA2) was used as electrode and the industry pure nitrogen gas as shielding and reacting atmosphere. The microstructures, interfacial behavior, phase and element in the coatings were investigated by scanning electronic microscope, X-ray diffraction and X-ray photo spectrum. The microhardness of coatings was tested and its wear-resistance property was tested by the self-made abrasion machine and compared with W18Cr4V rapid steel treated by quenching. The results show that an excellent bonding between the coating and substrate is ensured by the strong metallurgical interface. The coatings are mainly composed of Ti and synthesized TiN. The highest microhardness of coating reaches to 1 388 HV0.1, which is six times higher than that of the substrates. Wear resistance of the coatings is excellent.

Key words: reactive electric-spark deposition; TiN; composite coating; titanium alloy

Influence of transverse alternative magnetic field frequency on microstructure and properties of plasma arc surfacing layer LIU Zhengjun, ZHAO Qian, CI Honggang, SU Yunhai (School of